

Substitution of Glu122 by glutamine revealed the function of the second water molecule as a proton donor in the binuclear metal enzyme, creatininase.

Kinuyo Yamashita^{1†}, Yoshitaka Nakajima^{1†}, Hayato Matsushita¹, Yoshiaki Nishiya², Ryuji Yamazawa¹, Yu-fan Wu¹, Futoshi Matsubara¹, Hiroshi Oyama¹, Kiyoshi Ito^{1*}, and Tadashi Yoshimoto¹

¹Graduate School of Biomedical Sciences, Nagasaki University, 1-14 Bunkyo-machi, Nagasaki 852-8521, Japan, ²Tsuruga Institute of Biotechnology, Toyobo, Co. Ltd. 10-24 Toyo-cho, Tsuruga, Fukui 914-0047, Japan

*Corresponding author

†First two authors (K. Y., and Y. N.) contributed equally to this work.

School of Pharmaceutical Sciences, Nagasaki University, 1-14 Bunkyo-machi, Nagasaki 852-8521, Japan

Tel: +95-819-2435, Fax: +95-819-2478;

E-mail: k-ito@nagasaki-u.ac.jp

Running title: Creatininase from *P. putida*

SUMMARY

Creatininase is a binuclear zinc enzyme and catalyzes the reversible conversion of creatinine to creatine. It exhibits an open-closed conformational change upon substrate binding and the differences in the conformations of Tyr121, Trp154, and the loop region containing Trp174 were evident in the enzyme-creatine complex when compared to those in the ligand-free enzyme. We have determined the crystal structure of the enzyme complexed with a 1-methylguanidine. All subunits in the complex existed as the closed form, and the binding mode of creatinine was estimated. Site-directed mutagenesis revealed that the hydrophobic residues that show conformational change upon substrate binding are important for the enzyme activity.

We propose a catalytic mechanism of creatininase in which two water molecules have significant roles. The first molecule is a hydroxide ion (Wat1) that is bound as a bridge between the two metal ions, and attacks the carbonyl carbon of the substrate. The second molecule is a water molecule (Wat2) that is bound to the carboxyl group of Glu122 and functions as a proton donor in catalysis. The activity of the E122Q mutant was very low and it was only partially restored by the addition of $ZnCl_2$ or $MnCl_2$. In E122Q mutant, k_{cat} is drastically decreased, indicating that Glu122 is important for catalysis. X-ray crystallographic study and the atomic absorption spectrometry analysis of the E122Q mutant-substrate complex revealed that the drastic decrease of the activity of the E122Q was caused by not only the loss of one Zn ion at the Metal1 site but also a critical function of Glu122, which most likely exists for a proton transfer step through the Wat2.

Keywords: creatininase; binuclear metal center; amidohydrolase superfamily; catalytic mechanism; crystal structure

INTRODUCTION

Creatininase (creatinine amidohydrolase: [EC 3.5.2.10]) is a binuclear zinc enzyme that is closely related to the urease-related amidohydrolase superfamily and catalyzes the reversible conversion of creatinine to creatine. This reaction is the first step of the creatinine-metabolizing pathway found in *Pseudomonas putida* (1). Creatine is then degraded by creatinase [EC 3.5.3.3] (2), sarcosine dehydrogenase [EC 1.5.3.1] (3), and formaldehyde dehydrogenase [EC 1.1.1.159] (4) in this microorganism.

In mammals, creatinine is derived from creatine and creatine phosphate. A substantial amount of creatine phosphate is stored as a source of high-energy phosphoryl groups in muscle. With expanding ATP consumption, creatine kinase regenerates ATP from ADP and creatine phosphate. Creatinine is non-enzymatically produced at a constant rate, while creatine phosphate is reproduced enzymatically. Creatinine filtered out of the blood by the glomeruli in the kidney is excreted into urine without tubular reabsorption. Since the creatinine concentration in plasma is proportional to individual muscle mass, the creatinine clearance estimated from blood and urinary creatinine levels is important for renal function evaluation. At the present time, the creatine content is usually determined by an enzymatic method using creatininase, creatinase, and sarcosine oxidase.

Creatininase was first purified from *P. putida* as a creatinine-degrading enzyme (1). Later, it was found that the enzyme activity was increased approximately 4-fold by the

addition of manganese (5). The gene encoding creatininase was cloned from *P. putida* and over-expressed using an *E. coli* system (6). Sequences with a 30% or higher identity to *P. putida* creatininase, including sequences from *Arthrobacter sp.*, can be found in some bacterial genomes (7), although most of them have not been experimentally proven to show creatininase activity. The recombinant enzyme can be activated with manganese, and an Mn-activated enzyme has been applied for the diagnostic analysis of creatinine together with other creatinine-metabolizing enzymes. The three-dimensional structures of these enzymes have been reported (8-15).

We have determined the structures of the wild-type and Mn-activated enzymes. Two metal ions have been found at an active site in each subunit; two zinc ions in the wild-type enzyme. It is known that, one of the two ions is replaced with manganese in the Mn-activated enzyme. In dihydroorotase [EC 3.5.2.3] (16), isoaspartyl dipeptidase [EC 3.4.19.5] (17), and D-aminoacylase [EC 3.5.1.81] (18), which possess binuclear metal-center like creatininase, the water molecule bridging the metal ions initiates the catalytic reaction as a nucleophile (16-21). This water molecule forms a hydrogen bond with an Asp residue that is conserved in these enzymes and is coordinated with one of the metal ions (Metal1). It has been reported that the Asp residue functions as a catalytic base/acid at the ring-opening reaction through mediation of the proton from the water molecule to the product amino group. In the creatininase, however, the Wat1 is too far away from the acidic residues Glu34 and Asp45 coordinating with the Metal1 to form a hydrogen bond, although the bridging water molecule, Wat1, also acts as the nucleophile. On the other hand, the residue His178 is located at a position that allows it to form a hydrogen bond with the Wat1. It is considered, however, that the His178 is also not a proton donor for the catalytic reaction because it is at too great a distance

from the substrate. We have proposed a novel mechanism in which a water molecule, Wat2, which is coordinated to the Metal1 and forms a hydrogen bond with Glu122, functions as the proton donor (14).

From the structure determination of the creatininase, we also found a significant conformational change in the loop composed of Lys158-His178, indicating an open-closed conformational change upon substrate binding and that the creatinine or creatine were trapped in the active site as shown in Fig. 1 (14). As a result, the creatine is kept away from the solvent. It must be important for the catalytic reaction that the substrate is kept tightly in the closed active site.

In this study, we determined the crystal structure of creatininase complexed with an inhibitor, 1-methylguanidine, to estimate the details of the substrate recognition. The site-directed mutants of Y121A, W154A, W154F, W174A, and W174F were prepared to clarify the functions of hydrophobic residues around the active site in the open-closed conformational change upon substrate binding. Furthermore, the gene of the E122Q mutant was prepared to clarify the function of the Wat2. Finally, we discussed the functions of these residues in the catalytic reaction based on an enzyme-activity assay and the crystal structures of the mutants.

RESULTS

Site-directed mutagenesis

Six amino acid residues of Tyr121, Glu122, Trp154, Trp174, His178, and Glu183 were selected for site-directed mutagenesis. Conformational shifts of the side chains of Tyr121 and Trp154 are observed in the enzyme-creatine (reaction product) complex,

which allow the chains to make hydrophobic contact with creatine upon its binding. There is also a shift of the main chain of Trp174 upon creatine binding. Glu183 is a ligand of metal ion. His178 and Glu122 form hydrogen bonds with Wat1 and Wat2, respectively (Fig. 1). These residues were well conserved among the homologous sequences found by a BLAST search performed with the amino acid sequence of *P. putida* creatininase, except Tyr121, which was moderately conserved and tyrosine or phenylalanine was found at this position in some sequences.

All substitutions (Y121A, E122Q, W154A, W154F, W174A, W174F, H178A and E183Q) were confirmed by DNA sequencing and all the mutant *cre* genes were expressed at a high level similar to that achieved for the wild-type enzyme under the standard condition.

Binuclear metal center

Since the creatininase has a binuclear metal center, metal ion treatment was included in the standard purification procedure. The enzymes that received zinc treatment showed significantly higher activity than those without metal treatment and the use of manganese chloride increased the activity yield (Table 1). Our previous study revealed that two zinc ions and one zinc and one manganese ion were coordinated in the active site of the zinc-treated and the manganese-treated enzymes, respectively. The zinc content of the zinc-treated enzyme was determined to be 2.2 zinc molecules per subunit by atomic absorption spectrometry and this enzyme was designated as the wild-type enzyme (Zn-Zn). In order to investigate the effect of metal ions, we tried to remove the zinc ions by dialyzing against buffers containing *o*-phenanthroline. However, only a partial decrease (10-30%) in activity and zinc content were observed. Then we

prepared the enzyme from the cell-free extracts without zinc treatment and the purification was carried out using buffers containing EDTA throughout the procedure to remove metal ions from the enzyme. The zinc content of this enzyme preparation was 0.6 molecules per subunit. The specific activity was 178 units/mg, which was 48% of the activity of the wild-type enzyme (Zn-Zn); 370 units/mg. Although it was difficult to prepare a metal-free apoenzyme, we designated this enzyme preparation as semi-apoenzyme (Zn).

The wild-type enzyme (Zn-Zn) and the semi-apoenzyme (Zn) were preincubated with metal ions as described in the Materials and Methods and the activity was measured. The results were summarized in Table 2. The preincubation with ZnCl_2 had no effect on the activity of wild-type enzyme (Zn-Zn) and that with MnCl_2 increased the activity by 1.7-fold. The activity of the semi-apoenzyme (Zn) was fully restored by the incubation with ZnCl_2 . Furthermore, the activity of the semi-apoenzyme (Zn) after preincubation with MnCl_2 showed a comparable level of activity obtained for the wild-type enzyme purified from the cell-free extract treated with MnCl_2 . The specific activities and k_{cat} values of the wild-type enzyme (Zn-Zn) and the semi-apoenzyme (Zn) are closely related to their metal contents. The manganese activation was mainly due to the increase in k_{cat} , and the K_{m} values were not substantially changed.

The zinc content was measured for the E122Q mutant because the electron density corresponding to only one metal ion was observed in the crystal structure of this mutant, as described in detail below. The zinc content in the E122Q mutant was determined to be 0.85 molecules per subunit. The incubation with ZnCl_2 significantly increased the activity, indicating that the metal affinity of this mutant was weakened. In addition, the incubation with MnCl_2 resulted in a further increase in activity, showing significant

manganese activation on this mutant, although the absolute activity values were very low. When assay was performed in the presence of varying concentrations of metal chloride, the maximum activity was observed with 10 μM ZnCl_2 and 50 μM MnCl_2 for the wild-type enzyme. A little higher concentration was needed to obtain the maximum activity for the E122Q mutant enzyme than for the wild-type in our assay condition, suggesting that the metal affinity of the E122Q mutant enzyme was somewhat reduced.

Kinetic analysis of the wild-type and mutant enzymes

The kinetic constants for the wild-type and mutant creatininases are summarized in Table 1. All the mutations introduced at the 6 amino acid residues drastically decreased the activities of the mutant enzymes, except W174F, which retained approximately 47% of the activity of the wild-type enzyme (Mn-Zn). No activity was observed for the W154A, H178A and E183Q mutants. The Y121A and E122Q mutants showed 4.6% and 0.03% of the activity of the wild-type enzyme (Zn-Zn), respectively. The activity of the E122Q mutant was partially recovered by the addition of metal ions as described above.

On the mutations in two Trp residues, alanine substitution had a stronger effect than phenylalanine substitution. No and little activity was detected in W154A and W174A mutants, respectively. W174F mutant retained a level of activity comparable to the wild-type enzyme (Mn-Zn), and significant activity was observed for W154F mutant.

Crystal structure of the enzyme-1-methylguanidine complex

The enzyme-inhibitor complex was obtained by using a competitive inhibitor, 1-methylguanidine. In all subunits, 1-methylguanidine was found in the active site, as shown in Fig. 2a. The structure of the enzyme-inhibitor complex including the loop

region from Pro160 to His178 was closer to that of the enzyme-substrate complex displaying the closed form (PDB code: 1V7Z) rather than that of the wild-type enzyme (Mn-Zn) in the open form (PDB code: 1J2T) as shown in Fig. 2b. In the enzyme-inhibitor complex, the 1-methylguanidine, which shares a part of a creatine molecule, was bound in a similar way as observed for creatine. The 1-methylguanidine was not coordinated with the metal ions but was bound by forming a hydrophobic interaction with Tyr121 and Trp154, and hydrogen bonds with the main-chain carbonyl groups of Ser78, Trp174, and Asp175 with distances of 2.7, 2.8, and 2.8 Å, respectively. There was a difference of 21.1° in the angle between the guanidine planes of creatine and 1-methylguanidine bound at the active site (Fig. 2c). Two metal ions, Mn and Zn, are located at the active site, and three water molecules, Wat1, Wat2, and Wat3, are coordinated to metal ions as well as the wild-type enzyme (Mn-Zn).

Crystal structures of the W154A, W154F, and W174F mutants

Two structures of W174F mutant were determined using crystals with different space group; W174F- $P2_1$ and W174F- $P3_221$ at 2.0 and 1.78 Å resolution, respectively. The structures of W174F- $P2_1$ and W174F- $P3_221$ were almost identical with an rms deviation of 0.21 Å. We are going to discuss the structure of W174F mutant using the W174F- $P2_1$. Structural comparisons with the open and closed form showed that the W174F mutant possesses the open form structure (Fig. 3a). The active-site structure of the W174F mutant is shown in Fig. 4. Two metal ions of Mn and Zn are located at the active site of the W174F mutant, and a cacodylate anion is bound to these metal ions as shown in Fig. 5a. Two oxygens of the cacodylate anion were located at the positions corresponding to Wat1 and Wat3 in the wild-type enzyme (Mn-Zn), and two oxygens

formed hydrogen bonds with His178 and the main-chain NH group of Tyr121 at distances of 2.8 and 2.6 Å, respectively. The Wat2 was coordinated to the Mn ion at a distance of 2.1Å, and formed a hydrogen bond with Glu122 at a distance of 2.75 Å. Based on the observation of an open-closed conformational change upon substrate binding, Trp174, which is located in the loop region at a distance of 5.3 Å from Trp154, moves to cover the active-site pocket and undergoes a hydrophobic interaction at a distance of 3.4 Å. The Trp174 forms a hydrophobic contact with Phe171 in the same loop region at a distance of approximately 3.5 Å. Although the W174F mutant adopts the open form with respect to the main-chain structure, the side chain of Phe174 was located at a distance of 4.6 Å from Trp154 and occupied an intermediate position between the open and closed forms. Additionally, the distance between Phe171 and Phe174 was longer than that between Phe171 and Trp174 in the wild-type enzyme.

The structure of the W154A mutant was determined at the 2.0 Å resolution. The subunit structure of W154A mutant was closer to the open form (Fig. 3b). The high peak found at the corresponding position of the Wat1 was assigned as a chloride ion. The active-site structure of W154A mutant is shown in Fig. 4. Since Trp154 is one of the residues composing the active site pocket, the replacement to Ala resulted in wide exposure of the active site to the solvent.

The structure of W154F mutant was determined at 2.0 Å resolution. The 6 subunits of W154F mutant can be divided into two groups: a group that includes subunits A, B, and C, and a group that includes subunits D, E, and F. The structures of both subunits A and D were closer to open form, but the structures of Val150-His178 containing the loop region were significantly different from each other (Fig. 3b). It was considered that the difference in conformation between these subunits was related to the conformational

change of Phe154. As shown in Fig. 4, the conformation of Phe154 in the subunit A was similar to that in the wild-type enzyme (Mn-Zn). As shown in Fig. 3b, the side chain phenyl ring of Phe154 was located at the center position of the indole ring of Trp154 in the wild-type enzyme (Mn-Zn). The structure of Val150-His178 was virtually identical to that in the open form, even though the electron density map of Glu169-Asp175 in the subunit A was comparatively obscure; the models of these regions were built as poly-Ala models. Meanwhile, the conformation of Ph154 in the subunit D was unique, as shown in Fig. 4. The side chain χ_1 angle of Phe154 changed to -79.3° from 48.1° in the subunit A, and the position of C α was altered by 1.14 Å from that in the subunit A. Consequently, Phe154 was accommodated into the hydrophobic pocket composed of Tyr153, Phe182, and Trp174. It was considered that this unique conformation of Phe154 affected the main-chain structure of Val150-His178. A manganese and a zinc ion are found at the active site in all subunits, and three water molecules, Wat1, Wat2, and Wat3, are conserved as well as the wild-type enzyme (Mn-Zn), as shown in Fig. 5b.

Crystal structures of the E122Q mutants

In our previous paper, we hypothesized that Wat2 acts as a catalytic acid and a proton donor. The structure of the E122Q mutant was determined at 2.0 Å resolution. The subunit structure was almost identical to that of the closed form (Fig. 3c). The difference Fourier map corresponding to creatine was displayed at the active site of five subunits in the hexamer. Only one peak corresponding to zinc ion was found in the active site of this complex, the E122Q (Zn)-substrate complex. This result agreed with the zinc content (0.85 Zn/subunit) estimated from the atomic absorption spectrometry. A zinc ion (Metal2) coordinated with His36, Asp45 and Glu183 was identified in the

crystal structure but the other zinc ion (Metal1) that is bound to Glu122 through a hydrogen bond with Wat2 was not found (Fig. 5c). It was suggested that the negative charge on Glu122 is essential to bind a metal ion at the Metal1 site. The active site of the E122Q (Zn)-substrate complex is shown in Fig. 6. The active-site structure of the E122Q (Zn)-substrate complex is quite similar to that of the wild-type except for the occupied state of Metal1, the side-chain conformation of the 122nd residue, and the positions of Wat2 and creatine. In the wild-type enzyme (Mn-Zn), the conformation of Glu122 is stabilized by two hydrogen bonds of the side chain with main-chain NH group of Gln75 and itself. In the E122Q (Zn)-substrate complex, meanwhile, only a hydrogen bond between Gln122 and Gln75 was formed. A different hydrogen-bonding network may be responsible for the conformational change of Gln122. The position of Wat2 in the E122Q (Zn)-substrate complex is 0.88 Å away from that in the enzyme-substrate complex, and the distance between creatine and Wat2 in the E122Q-substrate complex (3.10 Å) differs little from that in the enzyme-substrate complex (3.04 Å). The hydrogen bond between Wat2 and Gln122 is 2.92 Å, which is 0.26 Å longer than that between Wat2 and Glu122 in the enzyme-substrate complex.

The structure of E122Q mutant crystallized in the presence of MnCl₂, the E122Q (Mn-Zn) mutant was determined at 2.2 Å resolution. The structure of the loop region was somewhat closer to that in the open form; however, the loop was located at an intermediate position between the open and closed form (Fig. 3c). The active-site structure of E122Q (Mn-Zn) mutant is shown in Fig. 6. In the active site of E122Q (Mn-Zn) mutant, two high peaks on the difference map were found at positions corresponding to the metal-binding sites, and these peaks were assigned as a manganese and a zinc ion. Additionally, an electron density map assigned as a chloride ion was

found on the binuclear metal center. The chloride ion was located at distances of 2.7, 3.0, and 3.8 Å from the manganese ion, zinc ion, and His178, respectively. Unlike the E122Q (Zn)-substrate complex, the conformation of Gln122, the electron density map of which was slightly obscure, was similar to that in the wild-type enzyme; the side chain of Gln122 faced the manganese ion. However, no peak corresponding to Wat2 was found around the manganese ion at the active site in any of the subunits (Fig. 5d).

The structure of E122Q mutant crystallized in the presence of ZnCl₂, the E122Q (Zn-Zn) mutant, was determined at 2.0 Å resolution. As shown in Fig. 3c, the structure of E122Q (Zn-Zn) mutant was closer to the closed form. It was considered that the closed form of E122Q (Zn-Zn) mutant was induced by the addition of creatinine during crystallization. Nevertheless, no electron density map that could possibly be assigned as creatinine or creatine was found at the active site. The active-site structure is shown in Fig. 6. Two zinc ions and a chloride ion were found at each subunit, and the chloride ion was located at distances of 3.0, 3.3, and 3.5 Å from the zinc ions on the Metal1 and Metal2, and His178, respectively. The electron density map of Gln122 remained obscure, and the side-chain conformation was disordered. Additionally, no electron density map corresponding to the Wat2 was found on the zinc ion at the Metal1.

DISCUSSION

The structure of the wild-type enzyme complexed with 1-methylguanidine was determined to exist as the closed form. The 1-methylguanidine was bound in the active site through hydrogen bonds with the main-chain carbonyl group of Ser78, Trp174, and Asp175 but was not coordinated with the metal ions. It is likely that these hydrogen

bonds contribute to the induction of the closed form. In addition, we focused on other hydrophobic residues, including Tyr121, Trp154, and Trp174, all of which showed conformational change upon creatine binding. The two Trp residues are located at the active site and underwent hydrophobic interactions with each other in the closed form. The Tyr121 approached the creatine by an induced fit and underwent a hydrophobic interaction with C α -C β of Asp175 on the loop region. The replacement of Tyr121 to Ala decreased the specific activity and k_{cat}/K_m value of the resultant Y121A mutant to 9.0% and 3.1% of that of the wild-type enzyme (Mn-Zn), respectively. The reduced activity is probably due to deficiency of the hydrophobic interaction between Tyr121 and Asp175. It is suggested that the Tyr121 is one of important residues for stabilization of the closed form

Based on the mutagenesis, both the Trp154 and Trp174 residues are important for the activity, but Trp154 is more critical and the substitution by a small Ala residue abolished the activity. The crystal structures of the W154A, W154F, and W174F mutants were determined. Trp154 is one of the residues composing the substrate-binding pocket at the active site. It is evident that the replacement of Trp154 to Ala broadly exposes the W154A mutant to the solvent. On three subunits of the W154F mutant, in which a hexamer is found in an asymmetric unit, Phe154 is located at the same position as Trp154 in the wild-type enzyme. On the other subunits, the side chain of Phe154 swung outward as if stacked on Tyr153 and Phe182. As a result, the activity of these subunits was likely to be lost because the active sites in the last three subunits were exposed to solvent as in the W154A mutant. Additionally, this conformation would restrict the conformational change of the loop region. If the first three subunits changed to the closed form upon substrate binding, it is expected that the substrate could be

accommodated in the protein molecule. However, a low activity of W154F was observed even in this situation, and this result could be explained as follows. In the first three subunits, the side chain of Phe154 was located at the center of the indole ring on Trp154 in the wild-type enzyme. An increased distance from Phe154 to Trp174 at the closed form of these subunits would reduce the hydrophobic interaction between these residues. In a similar fashion, the decreased activity of the W174F mutant can be explained by the reduced hydrophobic interaction between Trp154 and Phe174, which was caused by the replacement to a smaller Phe residue from the bulky Trp residue. Because the change in the distance between Trp154 and Phe174 in the closed conformation is expected to be small, however, the activity may be retained in the W174F mutant compared with the W154F mutant. From these results, it is considered that the hydrophobic residues around the active site are involved in the stabilization of the closed form through binding of the loop region by the hydrophobic interaction between them.

In the scheme proposed in Fig. 7, a catalytic mechanism would explain the ring-opening reaction of creatinine. The reaction would be initiated by the nucleophilic attack of the water molecule (Wat1), which is activated as a hydroxide ion by the binuclear metal center. The Wat1 attacks to the carbonyl carbon of the creatinine to form a tetrahedral intermediate. In the second step, the carbon-nitrogen bond of the intermediate is cleaved with receiving a proton from the water molecule (Wat2) bound to Glu122. Herein, the product, creatine, is bound to the binuclear metal center through the carboxyl group. The enzyme can turn over by releasing a product with the conformational change, and recoordination and activation of a water molecule (Wat1) takes place on the binuclear metal center.

The 1-methylguanidine was bound to the active site in the same fashion as the creatine. However, the plane of the 1-methylguanidine was not superimposed on the position of the 1-methylguanidyl portion of the creatine (Fig. 2c). A model of a creatinine complex was built by superimposing a creatinine onto the 1-methylguanidine. In this model, the carbonyl oxygen of the creatinine would be coordinated to the Metal1 and the carbonyl carbon would be located at a position suitable to receive the nucleophilic attack, indicating that the model is consistent with our proposed catalytic mechanism and that it adequately reflects the structure of the enzyme-creatinine complex.

In the present study, we suggested that two water molecules (Wat1 and Wat2) had a critical function in the catalytic reaction. The first step in our proposed mechanism is the same as the nucleophilic attack by the hydroxide ion (Wat1) in the proposed mechanism of the urease-related amidohydrolase superfamily (14). In the mechanism of creatininase, however, the second step was different from that in the superfamily enzymes, which include dihydroorotase [EC 3.5.2.3], isoaspartyl dipeptidase [EC 3.4.19.5] and D-aminoacylase [EC 3.5.1.81]. In these enzymes, it has been reported that the conserved Asp residue acts directly as a proton donor for the bond cleavage reaction (16-18). No residue corresponding to this Asp is conserved in creatininases. We propose that the water molecule (Wat2), which coordinated to Mn and formed a hydrogen bond with Glu122, would act as a proton donor in the catalytic reaction.

In order to clarify the functions of the Wat2 and Glu122, Glu122 was replaced by glutamine by site-directed mutagenesis. The specific activity of the E122Q (Zn) mutant was less than 0.1% of that of the wild-type enzyme (Zn-Zn). From the crystal structure of the E122Q (Zn)-substrate complex, it was revealed that one of the binuclear metal

centers, Metal1, was deficient, indicating that the Glu122 is an important residue for tight binding of the Metal1 ion to the active site and that the side-chain carboxyl group is likely to be deprotonated in the wild-type enzyme. As shown in Table 3, although the activity of E122Q mutant enzyme was very low, the same extent of manganese activation could be observed, indicating that the active site of this mutant was still related to that of the wild-type enzyme. The effect on K_m was small and the large decrease in k_{cat} was the major cause of the activity decrease. The high Fourier peaks were found at each active site of the E122Q mutants after the addition of either $MnCl_2$ or $ZnCl_2$. These positions were overlapped with the position of the Metal1 site in the wild-type enzyme. In both E122Q mutants (Mn or Zn), a high peak was found on the binuclear metal center and was assigned as a chloride ion. This ion would have been taken up into the active site together with a metal ion. Although the wild-type enzyme, purified in the presence of EDTA, showed only half the activity of the wild-type enzyme (Zn-Zn), the activity was recovered by the addition of $ZnCl_2$ or $MnCl_2$. Activity was measured in the presence of various concentrations of potassium chloride and no change in activity was observed with potassium chloride concentration up to 100 mM. It is considered that the chloride ion has no effect on the enzyme activity and the drastic decrease in the activity of E122Q mutant is caused by a reason other than this chloride ion.

The Fourier peak corresponding to the Wat2 was not found at the active site in the E122Q mutant that contained two metal ions. Although the conformation of Gln122 in the E122Q (Zn)-substrate complex was different from that of the wild-type enzyme, the Gln122 in the E122Q (Mn-Zn) mutant would try to adopt the same conformation as in the wild-type enzyme upon binding the Metal1 to the active site. Because of the

intra-residual steric hindrance between the main-chain and side-chain amide groups, however, it would be difficult to form the same conformation as in the wild-type enzyme. Consequently, the E122Q mutant with two metal ions may lose the Wat2 from the active site. It is quite likely that the decreased activity of the E122Q mutant is caused by a deficiency of the Wat2 on the active site. The Wat2 is necessarily important in the catalytic reaction, and thus we conclude that the Glu122 and the Wat2 play critical roles.

MATERIALS AND METHODS

Materials

Restriction endonucleases, DNA modification enzymes, and a Mutan[®]-Super express Km kit were purchased from TaKaRa Shuzo (Otsu, Japan). The oligonucleotide primers containing the desired mutations were synthesized by Sigma Genosys Japan (Ishikari, Japan) and Genenet (Fukuoka, Japan). The BigDye terminator cycle sequencing kit and other reagents used for sequencing were obtained from Applied Biosystems Japan (Tokyo, Japan). Toyopearl HW65C, Toyopearl Butyl 650C, and DEAE-Toyopearl 650 were purchased from Tosoh (Tokyo, Japan). Creatinine, creatine, lithium sulfate monohydrate, and 1-methylguanidine were purchased from Nacalai Tesque, Inc. (Kyoto, Japan).

Bacterial strains, plasmids, and media

E. coli MV1184 (*ara*⁻, Δ (*lac-proAB*), *rpsL*, *thi*⁻, ϕ 80*dlacZ* Δ M15, Δ (*srl-recA*) 306: :Tn10, (F', *traD36*, *proAB*, *lacI*^q*lacZ* Δ M15)) was used for site-directed

mutagenesis. *E. coli* DH5 α (F⁻, ϕ 80 Δ lacZ Δ M15, Δ (lacZYA-argF) U169, *deoR*, *recA1*, *endA1*, *hsdR17* (r_k^- , m_k^+), *phoA*, *supE44*, λ^- , *thi-1*, *gyrA96*, *relA1*) and XL1-Blue (*recA1*, *endA1*, *gyrA96*, *thi-1*, *hsdR17*, *supE44*, *relA1*, *lac* [F['], *proAB*, *lacI*^q Δ M15, Tn10 (Tet^r)] were used for expression. Plasmids pKF19k and pUC19 were used for mutagenesis and expression. Bacteria were grown in Luria-Bertani broth (LB-broth).

Construction of the site-directed mutant gene

Two methods were used for site-directed mutagenesis. Construction of E122Q, W154A, H178A and E183Q mutants was carried out by using a Mutan[®]-Super Express Km kit according to the manufacturer's instructions. Mutagenic primers used were H178A: 5'-GGACATCGAGGCCGGCGGCGTC-3', E183Q: 5'-GGCGGCGTCTTGCAGACCTCCCTG-3', and W154F: 5'-GCTCTCCTACTTCGACTTCGTC-3'. Alternatively, the megaprimer-based PCR mutagenesis strategy (22) was used for the construction of Y121A, W154F, W174A and W174F. Flanking primers (*cre198-217s*: 5'- GCAAGCGGTCCGCCGAGCG-3' and *cre748-767a*: 5'- CCAGCATCCACGACCTTC-3') were used with mutagenic primers; E122Q: 5'-ACGGCCACTACCAAATTCCATG-3', W174A: 5'-GCTCTCCTACGCGGACTTCGTCA-3', W174A: 5'-TCCTCGGCGCGGACATCGAG-3', and W174F: 5'-TTCCTCGGCTTCGACATCGAG-3'. All the mutations were confirmed by sequencing and the mutant enzymes were expressed under essentially the same condition for the wild-type enzyme.

Purification of the wild-type and mutant enzymes

Expression and purification of the wild-type and mutant enzymes were carried out using the method described previously (14). For the Mn-activated wild-type enzyme and W154A, W154F, and W174F mutants, 1 M MnCl_2 solution was added to the supernatant to give a 8% (v/v) concentration before the protamine treatment. For the wild type enzyme (Zn-Zn), 1 M ZnCl_2 solution was used. The solutions containing metal chloride were stirred for 30 min at room temperature and then centrifuged (22540g, 30 min, and 4°C). The Toyopearl Butyl-650C column was substituted for the Toyopearl HW65C column. Enzymes adsorbed to the column were eluted with a linear gradient of 35% to 0% saturated ammonium sulfate in 20 mM potassium phosphate buffer (pH 7.5). The Y121A and E122Q mutant enzymes were purified using the same procedure without any metal treatment. For preparation of the apo-type of the wild-type enzyme, purification was carried out using the same buffers containing 10 mM EDTA throughout the purification procedure.

The purity of the enzymes was determined by SDS-PAGE. All enzyme solutions were dialyzed against 2 mM potassium phosphate buffer (pH 7.5) and concentrated using a Centriprep YM-30 (Millipore, Bedford, MA).

Atomic absorption spectrometry

Sample solutions for atomic absorption spectrometry were prepared with a wet digestion method. Up to 0.2 ml of enzyme solution was supplemented with 2.5 ml of concentrated nitric acid, then heated gradually to 140°C and kept at that temperature for 10 min. After allowing the solution to cool down to room temperature, 0.5 ml of perchloric acid was added to digest the sample, and then heated for 1 h at 140°C, for 30

min at 160°C, and finally for 15 min at 175°C. The solution was allowed to return to room temperature, and 0.5 ml of water was added. The solution was heated for 20 min at 140°C. Then the temperature was elevated to 170°C until white smoke appeared. This heating step with water was repeated again. The volume of the digested solution was adjusted to 10 ml by 0.1 M HCl. The zinc contents of the wild-type enzyme (Zn-Zn), semi-apoenzyme (Zn), and E122Q mutant enzyme were determined by a flame atomic absorption spectrometer AAnalyst 200 (Perkin Elmer, Foster City, CA).

Enzyme activity assay and kinetic studies

Enzyme activity was determined by measuring the amount of creatinine produced from creatine as a substrate using the Jaffe reaction (5, 14). The activity was estimated using a molar extinction coefficient of 4650 M⁻¹cm⁻¹ at 520 nm. To determine the K_m values, the creatine concentration was varied and Lineweaver-Burk plots were used to calculate K_m and the apparent V_{max} . The enzyme concentration was estimated based on a molar extinction coefficient of 28590 M⁻¹cm⁻¹ and a molecular weight of 27926, and the k_{cat} was calculated.

Effect of metal ions was investigated by preincubating the enzyme with metal ions before activity assay. The enzyme solutions were incubated for 15 min at room temperature in the presence of 0.1 mM ZnCl₂ or 0.1 mM MnCl₂ and the activity was determined by the standard protocol. Alternatively, assay was carried out in the presence of varying concentrations of metal chloride.

Crystallizations and X-ray data collections

Crystals of the enzyme-inhibitor complex were obtained by the hanging-drop

vapor-diffusion method at 20°C. A droplet was prepared by mixing an equal volume of 25 mg/ml Mn-activated enzyme solution and a reservoir solution containing 1.5 M lithium sulfate, 0.1 M HEPES buffer (pH 7.5), and 5 mM 1-methylguanidine. The E122Q (Zn)-substrate complex was crystallized by the sitting-drop vapor-diffusion method at 5°C using 50 mg/ml E122Q mutant enzyme solution and a reservoir solution containing 1.6 M lithium sulfate, 0.1 M HEPES buffer (pH 7.5) and 120 mM creatinine. The data of the enzyme-inhibitor complex and the E122Q (Zn)-substrate complex were collected using synchrotron radiation with a wavelength of 1.000 Å with a MAR CCD 165 detector at the BL41XU station of SPring-8 (Hyogo, Japan) and with an ADSC Quantum 4R detector at the BL6A station of the Photon Factory (Tsukuba, Japan), respectively. These crystals were isomorphous with those of the Mn-activated creatininase and its creatine complex (PDB code: 1J2T and 1V7Z, 14).

We screened for new conditions for the crystallization of W154A, W154F, and W174F mutants by the hanging-drop vapor diffusion method at 20°C using 25 mg/ml mutant-enzyme solution. Crystals were obtained with a reservoir solution containing 42-48% (v/v) PEG200, 10-20 mM MgCl₂, and 100 mM Na cacodylate buffer (pH 6.0) or 100 mM MES buffer (pH 6.0). Two kinds of crystals appeared under this condition; one was a plate-shaped crystal belonging to the space group $P2_1$, and the other was a partial merohedral twin crystal with a hexagonal-column shape belonging to the space group $P3_121$ or $P3_221$. The data of plate-shaped crystals for the W174F and W154A mutants were collected at the Photon Factory BL6A station and the data of twin crystals for the W174F and W154F mutants were collected with ADSC Quantum 315 and Quantum 210R CCD systems at the Photon Factory BL5A and the PF-AR NW-12 stations, respectively. A crystal of the E122Q mutant treated with MnCl₂ (E122Q

(Mn-Zn)) was obtained under the same conditions using PEG200 as the precipitant and 25 mg/ml enzyme solution containing 1 mM MnCl_2 . The data for this crystal were collected at the PF-AR NW12 station. Crystals of the E122Q mutant treated with ZnCl_2 (E122Q (Zn-Zn)) were also obtained under the same conditions. However, none of the data collected for these crystals were of sufficiently high quality. Therefore, crystals of E122Q (Zn-Zn) were obtained using 46-48% (v/v) PEG200, 10 mM MgSO_4 , 100 mM MES buffer (pH6.0), and 100 mM creatinine. The data were collected at the Photon Factory BL5A station.

The data of W154A were processed with the programs MOSFLM and SCALA in the CCP4 program suites (23), and the others were processed and scaled with the program HKL2000 (24). The statistics of crystallization conditions, crystallographic parameters, and data collection are summarized in Table 3.

Structure determinations and refinements

The model building was performed using the programs XTALVIEW (25) and COOT (26). The coordinate of Mn-activated creatininase was used for the initial model of the enzyme-inhibitor complex. The structure of the enzyme-inhibitor complex was refined by simulated annealing and energy minimization with the program CNS (27) using the data obtained from 20 to 1.9 Å resolution. No particular restraints for metal coordination were applied to the groups through the refinement procedure. The structure was examined by inspecting the composite omit map. The difference Fourier map clearly displayed a residual electron density corresponding to 1-methylguanidine bound at the active site. Refinement and model rebuilding were alternatively carried out over several cycles. Then water molecules were selected on the basis of the peak height and

the distance criteria from the difference Fourier map. Further model building and refinement cycles gave an R -factor of 19.2% and an R -free value of 20.7% using 203,364 reflections from 20 to 1.9 Å resolution. The maximal thermal factor of the water molecules was 50 Å². The same refinement procedure was applied to the E122Q (Zn)-substrate complex. Only one peak, which corresponds to one of two metal ions, was found in each active site from the difference Fourier map. Additionally, the difference map displayed a residual electron density corresponding to a creatine in the active site at five subunits of hexamer. From the results of model building and refinement cycles, the R -factor and R -free value decreased to 19.9% and 21.7%, respectively. The maximal thermal factor of the water molecules was 50 Å².

Two different crystals of the W174F mutant were obtained under the new conditions. One was a crystal belonging to space group $P2_1$ with the following cell constants: $a = 105.9$ Å, $b = 59.7$ Å, $c = 145.1$ Å, $\beta = 99.7^\circ$. One hexamer is found in an asymmetric unit of this crystal, and approximately 53% of the crystal volume is occupied by solvent. The crystal structure of the W174F mutant (W174F- $P2_1$) was determined by the molecular replacement method with the program PHASER in the CCP4 program suite (23) using the structure of the Mn-activated enzyme as the search model. The structure was refined with the program CNS (27) using the data obtained from 20 to 2.0 Å resolution. A residual density map on the binuclear metal center was clearly displayed at the active site of each subunit, and these were designated as a cacodylate anion by the corresponding tetrahedral shape, size, and peak, and the possible interactions of the peak with the enzyme. After addition of water molecules on the basis of residual peaks on the difference Fourier map, further model building and refinement cycles gave an R -factor of 19.6% and an R_{free} of 22.9%. The maximum thermal factor of the water

molecules was 59 \AA^2 . The other crystal is a partial merohedral twin crystal belonging to space group $P3_121$ or $P3_221$ with the following cell constants: $a = b = 164.3 \text{ \AA}$, $c = 163.9 \text{ \AA}$. One hexamer is found in an asymmetric unit, and approximately 67% of the crystal volume is occupied by solvent. The twin fraction was estimated to be 0.463 (28). The crystal structure was determined by the molecular replacement method with the program PHASER using the coordinates of 1J2T as the search model at the space group $P3_221$. A residual density map found at the active site in each subunit was designated a cacodylate anion. After several refinement and model building cycles using the same procedure as for W174F- $P2_1$, the structure of W174F- $P3_221$ was refined to decrease the R -factor to 23.5% and R -free value to 25.8% using diffraction data from 20 to 1.78 \AA resolution. The maximum thermal factor of the water molecules was 32 \AA^2 .

The structure of the W154A mutant was determined and refined with the same procedure using the coordinates of W174F- $P2_1$ as an initial model. In each active site, a high peak on the difference Fourier map was found. However, the position was slightly different from the cacodylate anion in W174F- $P2_1$. From the peak height and shape, this peak was designated as a chloride ion. After several refinement and model building cycles, the structure of the W154A mutant was refined to decrease the R -factor to 19.9% and the R -free value to 23.1% using diffraction data from 20 to 1.78 \AA resolution. The maximum thermal factor of the water molecules was 58 \AA^2 . The crystal structure of the W154F mutant with the space group $P3_221$ was determined and refined with the same procedure using the coordinates of W174F- $P3_221$ as an initial model by estimating the twin fraction of 0.397. From the difference Fourier map, a peak assigned as a water molecule was found on the center of the binuclear metal center. Further refinements and model building cycles were carried out, and the R -factor and R -free value of the model

were decreased to 19.9% and 21.6% using data from 20 to 2.0 Å resolution, respectively. The maximum thermal factor of the water molecules was 26 Å². The structures of the E122Q (Mn-Zn) and E122Q (Zn-Zn) mutants were determined and refined using the coordinates of W174F-*P*₃₂₁ as an initial model by estimating the twin fractions of 0.421 and 0.467, respectively. Unlike the E122Q (Zn)-substrate complex, two peaks corresponding to the binuclear metal center were found at each active site. A peak on the center of binuclear metal ions was designated as a chloride ion from the peak height and shape on the difference map. The structures of E122Q (Mn-Zn) and E122Q (Zn-Zn) mutants were refined to have an *R*-factor and *R*-free value of 20.6% and 23.6% at 2.2 Å resolution, and of 23.5% and 25.9% at 2.0 Å resolution, respectively. The maximum thermal factor of the water molecules was 42 and 34 Å², respectively.

The refinement statistics are summarized in Table 3. All diagrams are drawn with the program POVScript⁺ (29) and rendered with the program POV-Ray (<http://www.povray.org>).

PDB accession codes

The atomic coordinates and structure factors for the wild-type enzyme complexed with 1-methylguanidine, W174F mutant enzyme with the space group *P*₂₁ and *P*₃₂₁, W154F mutant enzyme, W154A mutant enzyme, E122Q (Zn) mutant enzyme complexed with creatine, E122Q (Mn-Zn) mutant enzyme, and E122Q (Zn-Zn) mutant enzyme (PDB codes: 3A6D, 3A6E, 3A6F, 3A6G, 3A6H, 3A6J, 3A6K, and 3A6L) have been deposited in the Protein Data Bank Japan, Osaka University (PDBj; <http://www.pdbj.org/>).

Acknowledgements

This work was supported in part by the Grant-in-Aid for Scientific Research from Japan Society for the Promotion of Science (JSPS). We thank Ms. K. Furukawa and Mr. M. Takeo for their excellent technical assistance. We are grateful to Dr. M. Haratake and Mr. M. Hongoh for the determination of metal contents by atomic absorption spectrometry.

REFERENCES

1. Tsuru, D., Oka, I., and Yoshimoto, T., (1976) Creatinine decomposing enzymes in *Pseudomonas putida*, *Agr. Biol. Chem.* **40**, 1011-1018.
2. Yoshimoto, T., Oka, I., and Tsuru, D., (1976) Creatine amidinohydrolase of *Pseudomonas putida*: crystallization and some properties. *Arch. Biochem. Biophys.* **177**, 508-515
3. Oka, I., Yoshimoto, T., Rikitake, K., Ogushi, S., and Tsuru, D., (1979) Sarcosine dehydrogenase from *Pseudomonas putida*: purification and some properties. *Agr. Biol. Chem.* **43**, 1197-1203.
4. Ando, M., Yoshimoto, T., Ogushi, S., Rikitake, K., Shibata, S., and Tsuru, D. (1979) Formaldehyde dehydrogenase from *Pseudomonas putida*: purification and some properties *J. Biochem.* **85**, 1165-1172.
5. Rikitake, K., Oka, I., Ando, M., Yoshimoto, T., and Tsuru, D. (1979) Creatinine amidohydrolase (creatininase) from *Pseudomonas putida*: purification and some properties, *J. Biochem.* **86**, 1109-1117.
6. Yamamoto, K., Oka, M., Kikuchi, T., and Emi, S. (1995) Cloning of the creatinine amidohydrolase gene from *Pseudomonas* sp. PS-7, *Biosci. Biotech. Biochem.* **59**,

1331-1332.

7. Nishiya, Y., Toda, A., and Oka, M., (2001) Characterization and structural prediction of the *Arthrobacter creatininase*. *J. Anal. Bio-Sci.* **24**, 144-149.
8. Hoeffken, H.W., Knof, S.H., Bartlett, P.A., Huber, R., Moellering, H., and Schumacher, G. (1988) Crystal structure determination, refinement and molecular model of creatine amidinohydrolase from *Pseudomonas putida*, *J. Mol. Biol.* **204**, 417-433.
9. Coll, M., Knof, S.H., Ohga, Y., Messerschmidt, A., Huber, R. Mollering, H., Russmann, L., and Schumacher, G. (1990) Enzymatic mechanism of creatine amidinohydrolase as deduced from crystal structures. *J. Mol. Biol.* **214**, 597-610.
10. Wagner, M.A., Trickey, P., Chen, Z-W., Mathews, .S. and Jorns, M.S., (2000) Monomeric sarcosine oxidase:1 Flavin reactivity and active site binding determinants, *Biochemistry* **39**, 8813-8824.
11. Zhao, G., Song, H., Chen, Z-W., Mathews, F.S., and Jorns, M.S. (2002) Monomeric sarcosine oxidase: role of histidine 269 in catalysis. *Biochemistry* **41**, 9751-9764.
12. Tanaka, N., Kusakabe, Y., Ito, K., Yoshimoto, T. and Nakamura, K.T (2002) Crystal structure of formaldehyde dehydrogenase from *Pseudomonas putida*: the structural origin of the tightly bound cofactor in nicotinoprotein dehydrogenases. *J. Mol Biol.* **324**, 519-533.
13. Ito, K., Kanada, N., Inoue, T., furukawa, K., Yamashita, K., Tanaka, N., Nakamura, K.T., Nishiya, Y., Sogabe, A., and Yoshimoto, T. (2002) Preliminary crystallographic studies of the creatinine amidohydrolase. *Acta Crystallogr. Sect. D Biol. Crystallogr.* **58**, 2180-2181.
14. Yoshimoto, T., Tanaka, N., Kanada, N., Inoue, T., Nakajima, Y., Haratake, M.,

- Nakamura, K., Xu, Y., and Ito, K. (2004) Crystal Structure of Creatininase Reveal the substrate Binding Site and Provide an Insight into the Catalytic Mechanism. *J. Mol. Biol.* **337**, 399-416.
15. Beuth, B., Niefind, K., and Schomburg, D. (2003) Crystal Structure of creatininase from *Pseudomonas putida*: a novel fold and a case of convergent evolution. *J. Mol. Biol.* **332**, 287-301.
16. Thoden, J. B., Phillips, G. N., Neal, T. M., Raushel, F. M., and Holden, H. M. (2001) Molecular structure of dihydroorotase: a paradigm for catalysis through the use of a binuclear metal center. *Biochemistry* **40**, 6989–6997.
17. Thoden, J. B., Marti-Arbona, R., Raushel, F. M., and Holden, H. M. (2003) High-resolution X-ray structure of isoaspartyl dipeptidase from *Escherichia coli*. *Biochemistry* **42**, 4874–4882.
18. Liaw, S.-H., Chen, S.-J., Ko, T.,-P. Hsu, C.-S., Chen, C.-J., Wang, A. H.-J. and Tsai, Y.-C. (2003) Crystal structure of aminoacylase from *Alcaligenes faecalis* DA1. *J. Biol. Chem.* **278**, 4957–4962.
19. Abendroth, J., Niefind, K., and Schomburg, D. X. (2002) X-ray structure of a dihydropyrimidinase from *Thermus* sp. at 1.3 Å resolution. *J. Mol. Biol.* **320**, 143–156.
20. Abendroth, J., Niefind, K., May, O., Siemann, M., Syltatk, C., and Schomburg, D. (2002) The structure of L-hydantoinase from *Arthrobacter aurescens* leads to an understanding of dihydropyrimidinase substrate and enantio specificity. *Biochemistry* **41**, 8589–8597.
21. Cheon, Y. H., Kim, H. K., Han, K. H., Abendroth, J., Niefind, K., Schomburg, D., Wang, J., and Kim, Y. (2002) Crystal structure of L-hydantoinase from *Bacillus*

- stearothermophilus*: insight into the stereochemistry of enantioselectivity. *Biochemistry* **41**, 9410–9417.
22. Tyagi R, Lai R, and Duggleby RG, (2004) A new approach to 'megaprimer' polymerase chain reaction mutagenesis without an intermediate gel purification. *BMC Biotechnol.* Feb 26;4:2.
 23. Collaborative Computational Project, Number 4 (1994), The CCP4 suite: programs for protein crystallography. *Acta Crystallogr. Sect. Biol Crystallogr.* **50**, 760-763
 24. Otwinoski, Z., and Minor, W. (1997) Processing of X-ray Diffraction Data Collected in Oscillation Mode, *Methods in Enzymology, Methods Enzymol.* **276**, 307-326
 25. McRee, D. E. (1999) XtalView/Xfit-A versatile program for manipulating atomic coordinates and electron density. *J. Struct. Biol.* **125**, 156-165
 26. Emsley, P. and Cowtan. K. (2004) Coot: Model-Building Tools for Molecular Graphics. *Acta Crystallogr. Sect. D Biol. Crystallogr.* **60**, 2126-2132
 27. Brunger, A. T., Adams, P. D., Clore, G. M., Delano, W. L., Gros, P., Grosse-Kunstleve, R. W., Jiang, J.-S., Kuszewski, J. N., Panni, N. S., Read, R. J., Rice, L. M., Simonson, T., and Warren, G. L. (1998) Crystallography and NMR System, a new software suite for macromolecular structure determination. *Acta Crystallogr. Sect. D Biol. Crystallogr.* **54**, 905-921
 28. Yeates, T. O. (1997) Detecting and overcoming crystal twinning. *Methods Enzymol.* **276**, 344-358
 29. Fenn, T. D., Ringe, D., and Petsko, G. A. (2003) POVScript⁺: a program for model and data visualization using persistence of vision ray-tracing. *J. Appl. Cryst.* **36**, 944-947

FIGURE LEGENDS

Fig. 1 Stereo diagram of the active site with the open-closed conformational change.

Structures of the active site superimposed between the wild-type creatininase (1J2T) in the open form and the creatine complex (1V7Z) in the closed form are shown as ribbon and stick models. The loop region, Tyr121 and Trp154 with different conformations between the open and closed form are represented by cyan and yellow, respectively.

Fig. 2 The active-site structure of the enzyme-inhibitor complex.

(a) Stereo diagram of the active site with the F_o-F_c omit map contoured at the 3σ level. The active site of the enzyme-inhibitor complex is shown as a ribbon and stick model. The electron density map was calculated by omitting structure factors from Mn, Zn, 1-methylguanidine, and three water molecules using diffraction data of 20-1.9 resolution. (b) Superimposed diagram of the three active sites. The loop region, Tyr121, and Trp154 involved in the conformational change at the wild-type enzyme (1J2T), the enzyme-substrate complex (1V7Z), and the enzyme-inhibitor complex are represented by cyan, yellow, and orange, respectively. Water molecules in the wild-type enzyme, the enzyme-substrate complex, and the enzyme-inhibitor complex are represented by red, yellow, and orange balls, respectively. (c) Side view of the active site superimposing the enzyme-inhibitor complex onto the enzyme-substrate complex. Stick models of creatine and 1-methylguanidine are represented by yellow and orange, respectively. The dihedral angle between the two guanidyl groups of these ligands was 21.1° .

Fig. 3 Stereo diagram superimposing the main-chain structures among the wild-type and mutant enzymes.

(a) Ribbon diagram of the structures of the enzyme-substrate complex (yellow), the W174F- $P2_1$ mutant (slate-blue), and the W174F- $P3_221$ mutant (blue) superimposed onto the wild-type enzyme (cyan). (b) Ribbon diagram of the structures of the enzyme-substrate complex (yellow), the W154A mutant (red), the W154F mutant-subunit A (pink), and the W154F mutant-subunit D (magenta) superimposed onto the wild-type enzyme (cyan). (c) Ribbon diagram of the structures of the enzyme-substrate complex (yellow), the E122Q (Mn-Zn) mutant (green), the E122Q (Zn-Zn) mutant (slate-grey), and E122Q (Zn)-substrate complex (dark-green) superimposed onto the wild-type enzyme (cyan).

Fig. 4 Stereo diagram superimposing active sites among the W174F, W154A, W154F mutants.

Active sites of subunit A in the W174F, W154A, and W154F mutants and subunit D in the W154F mutant are represented with slate-blue, red, pink, and magenta, respectively. In the subunit A of the W154F mutant, the conformation of Phe154 is almost the same as that of Trp154 in the wild-type enzyme or W174F mutant. However, Phe154 in the subunit D is accommodated into a hydrophobic pocket composed of Tyr153, Phe182 and Trp174 as a result of the conformational change.

Fig. 5 Stereo diagrams of the active center with the F_o-F_c omit map contoured at 2 sigma levels.

(a) Active site of the W174F mutant is shown by a ribbon and stick model. A cacodylate

anion is bound to the binuclear metal center, but the Wat2 is conserved and coordinated to the manganese. (b) Active site of the W154F mutant. Three water molecules, Wat1, Wat2 and Wat3, are bound to the active site as well as those in the wild-type enzyme. (c) Active site of the E122Q (Zn)-substrate complex. Peaks from one of two metal ions and creatine were displayed on the electron density map. Although the Wat2 was bound to the active site, the conformation of Gln122 was different from (d) that of E122Q (Mn-Zn) mutant.

Fig. 6 Stereo diagram of active sites in the E122Q mutants.

Active sites of the E122Q (Zn)-substrate complex, E122Q (Mn-Zn) mutant, and E122Q (Zn-Zn) mutant (c) are superimposed each other, and these are represented with dark-green, green, and slate-grey, respectively.

Fig. 7 Scheme of the proposed catalytic mechanism.

Figure 1

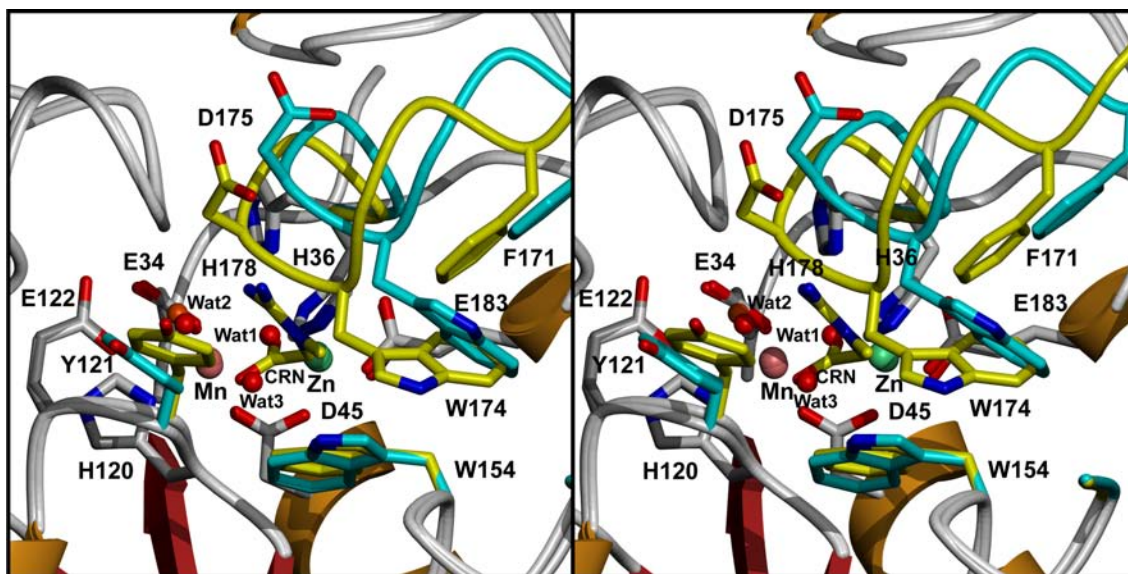
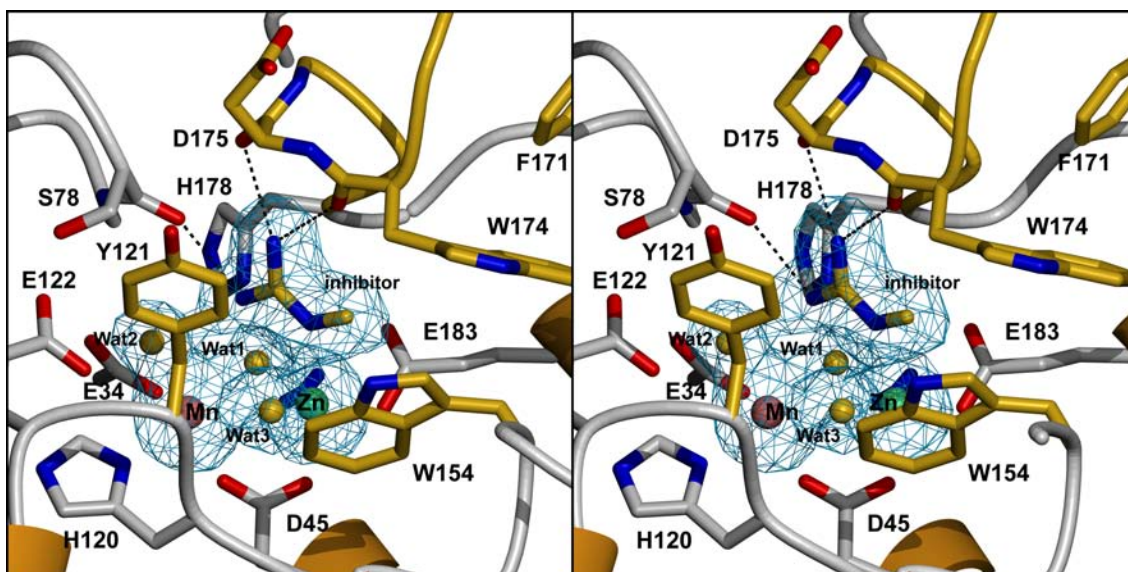
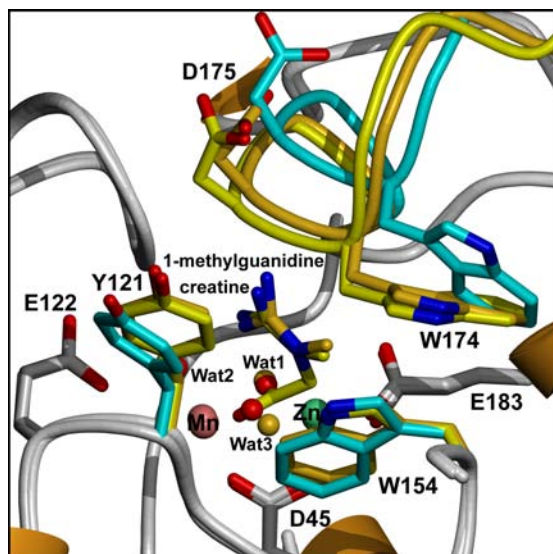


Figure 2

a



b



c

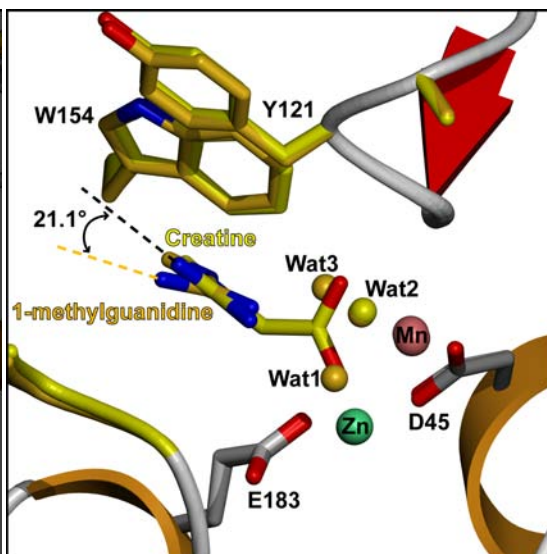
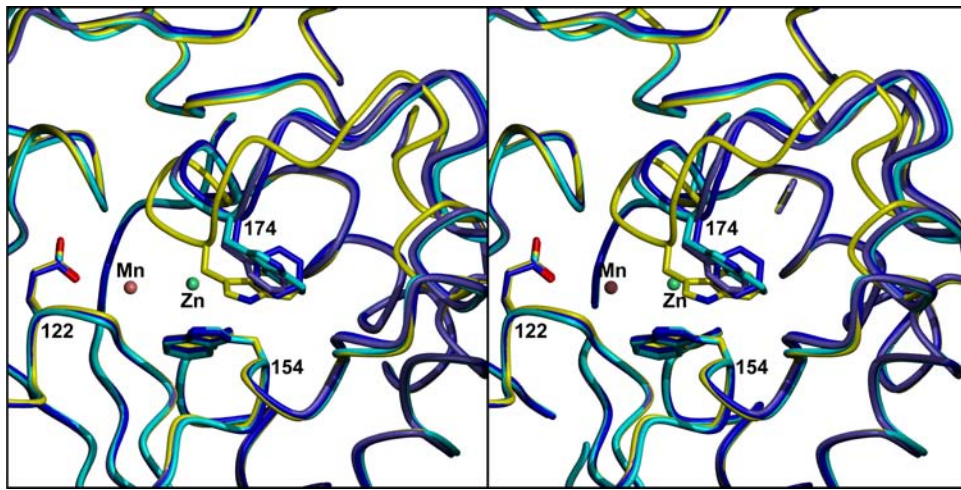
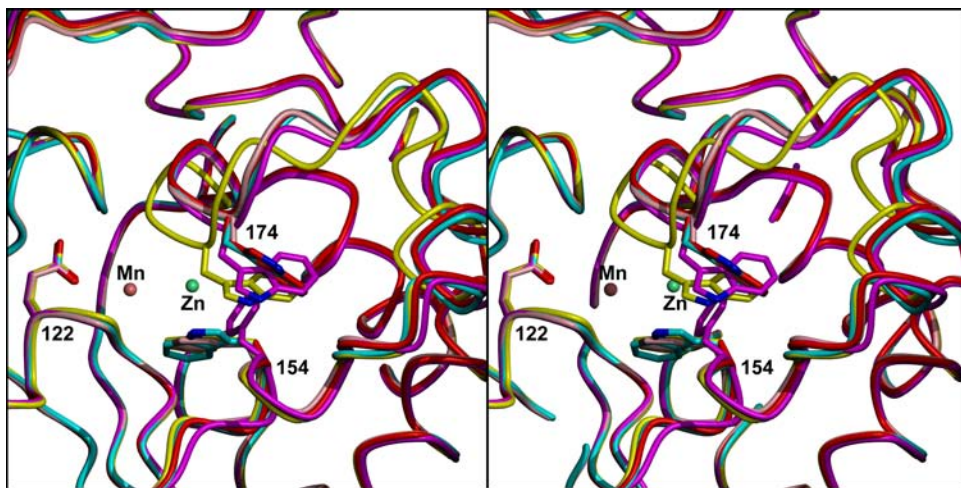


Figure 3

a



b



c

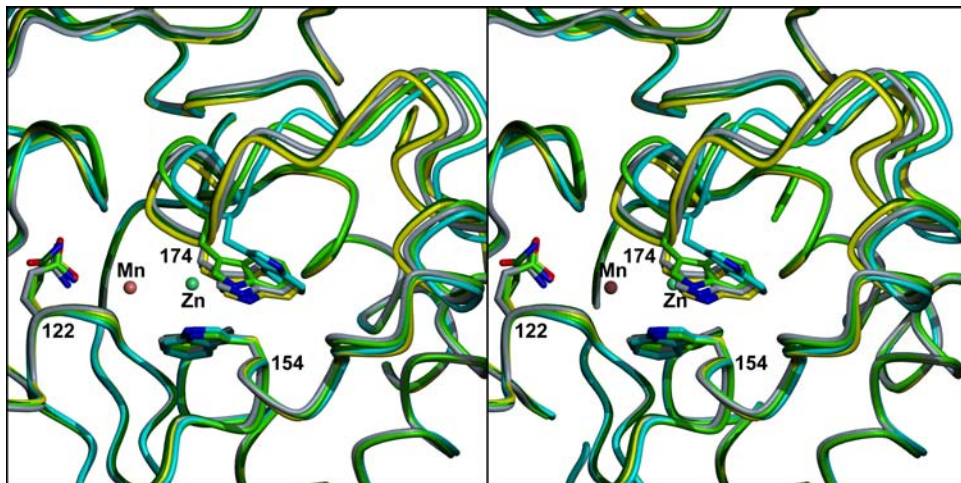


Figure 4

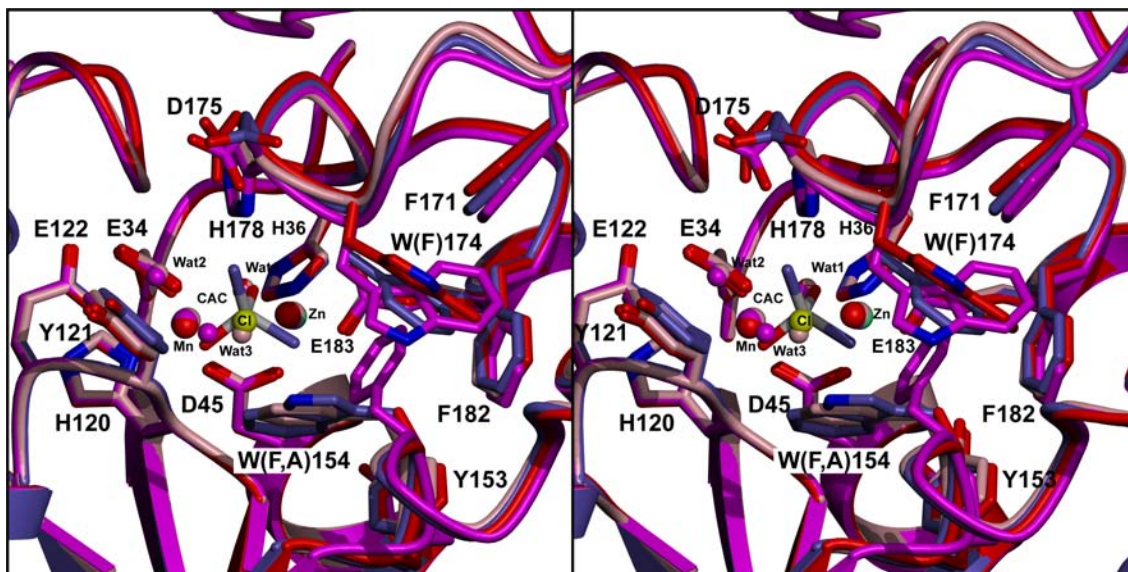
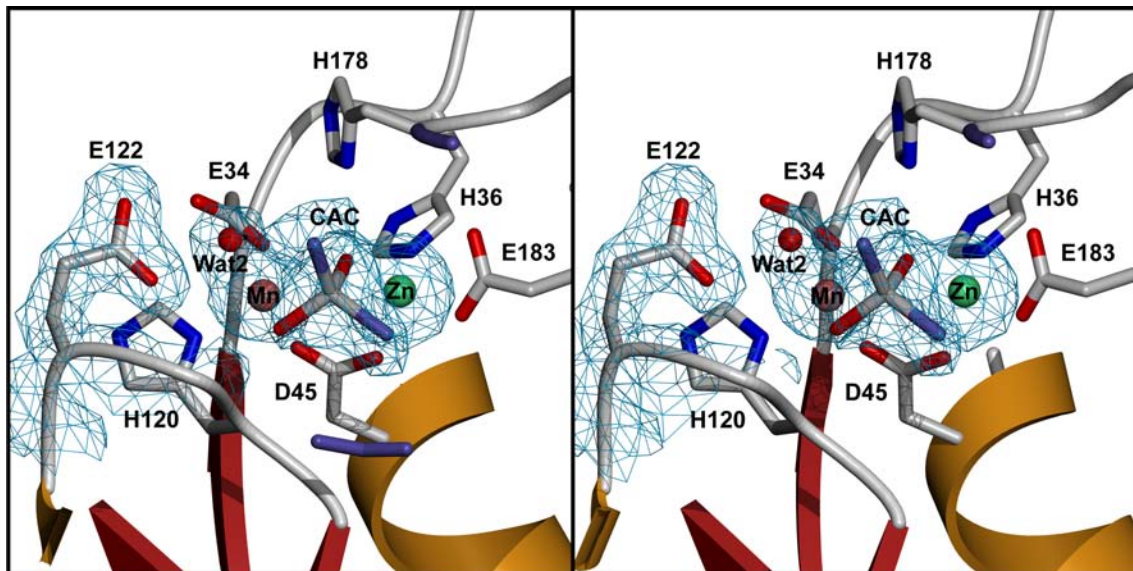
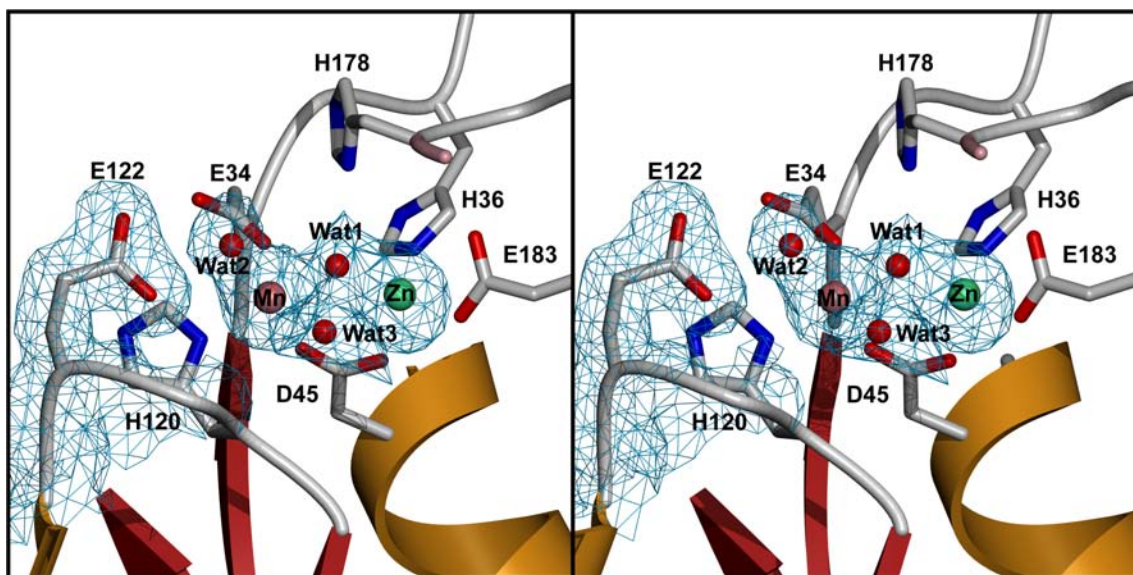


Figure 5

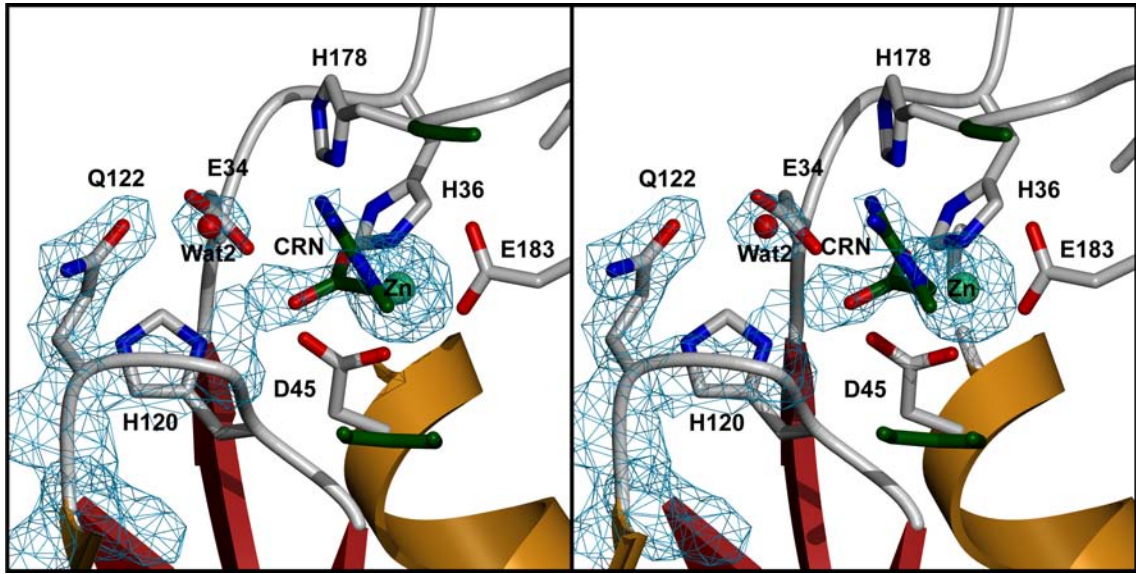
a



b



c



d

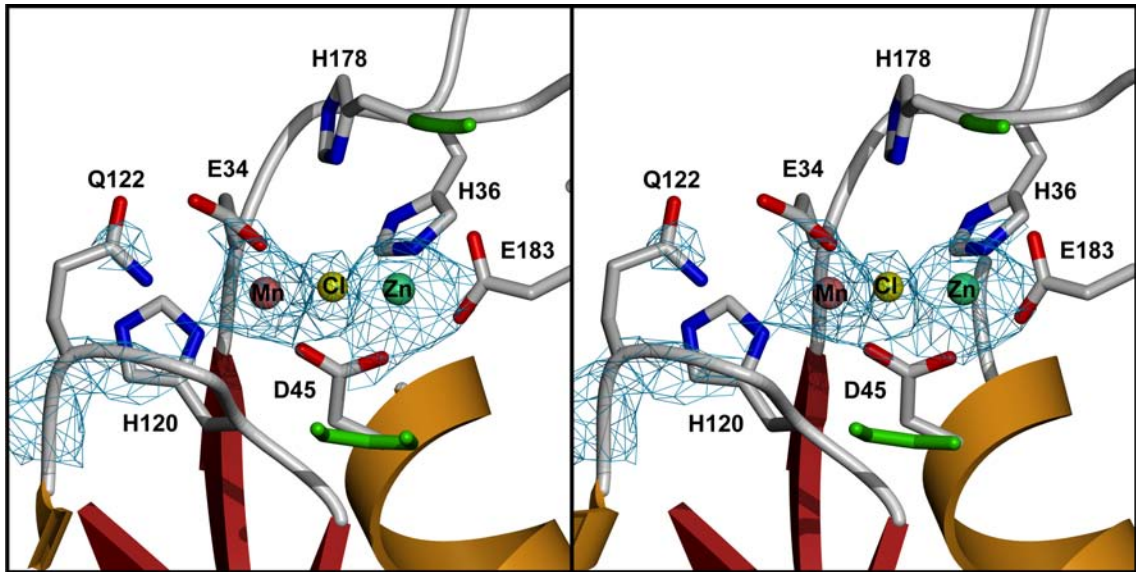


Figure 7

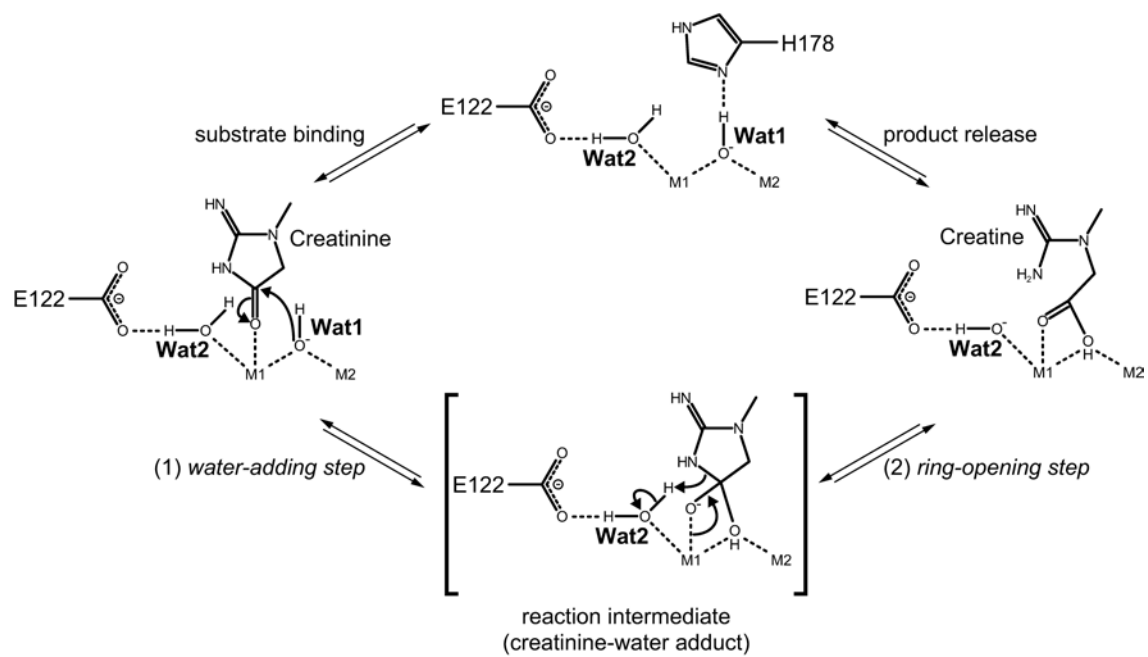


Table 1 Activities of the wild-type and various mutant creatininases.

Enzyme	Treatment ¹	Specific activity (units/mg)	Kinetic parameters		
			K_m (mM ⁻¹)	k_{cat} (sec ⁻¹)	k_{cat}/K_m (mM ⁻¹ sec ⁻¹)
Wild-type	ZnCl ₂	370 ± 4	44	252	5.73
	MnCl ₂	1560 ± 10	77	1340	17.4
(semi-apo)	EDTA ²	178 ± 8	150	222	1.48
Y121A	MnCl ₂	140 ± 1.2	160	86	0.54
E122Q	ZnCl ₂	0.13 ± 0.03	220	1.5	0.008
W154A	MnCl ₂	No activity	-	-	-
W154F	MnCl ₂	4.9 ± 0.3	350	178	0.51
W174A	MnCl ₂	Very low activity	-	-	-
W174F	MnCl ₂	740 ± 2	90	688	7.64
H178A	MnCl ₂	No activity	-	-	-
E183Q	MnCl ₂	No activity	-	-	-

¹Either ZnCl₂, or MnCl₂ was added to the crude extracts before the addition of protamine sulfate as described in the materials and methods. ²EDTA was included in all the buffers used for this enzyme preparation as described in the materials and methods. Activity assay was carried out with creatine as a substrate and the creatinine formed was determined by the Jaffe method.

Table 2 Effect of metal ions on the activity of the wild-type and the E122Q mutant creatininases.

Enzyme	Metal treatment							
	ZnCl ₂				MnCl ₂			
	Specific activity (units/mg)	<i>K_m</i> (mM ⁻¹)	<i>k_{cat}</i> (sec ⁻¹)	<i>k_{cat}/K_m</i> (mM ⁻¹ sec ⁻¹)	Specific activity (units/mg)	<i>K_m</i> (mM ⁻¹)	<i>k_{cat}</i> (sec ⁻¹)	<i>k_{cat}/K_m</i> (mM ⁻¹ sec ⁻¹)
wild-type enzyme (Zn-Zn)	376 ± 2	46	264	5.74	640 ± 38	46	437	9.5
semi-apoenzyme (Zn)	445 ± 9	32	280	8.75	1661 ± 41	70	1380	19.7
E122Q	3.1 ± 0.2	77	2.9	0.04	13.9 ± 0.6	56	11	0.20

Table 3 Data collection and Refinement statistics.

Data set	enzyme-inhibitor complex	W174F mutant	W174F mutant	W154F mutant	W154A mutant	E122Q (Zn) -substrate complex	E122Q (Mn-Zn) mutant	E122Q (Zn-Zn) mutant
PDB code	3A6D	3A6E	3A6F	3A6G	3A6H	3A6J	3A6K	3A6L
Data Collection								
X-ray source	SPring-8 BL41XU	PF BL6A	PF BL5A	PF AR-NW12	PF BL6A	PF BL6A	PF AR-NW12	PF BL5A
Wavelength (Å)	1.000	1.000	1.000	1.000	1.000	1.000	1.000	1.000
Space group	$P2_12_12_1$	$P2_1$	$P3_221$	$P3_221$	$P2_1$	$P2_12_12_1$	$P3_221$	$P3_221$
Cell parameter								
a (Å)	102.4	105.9	164.3	164.5	106.8	102.2	164.2	164.4
b (Å)	152.7	59.7	(164.3)	(164.5)	60.2	152.7	(164.2)	(164.4)
c (Å)	167.5	145.1	163.9	164.1	146.2	166.9	164.7	164.6
		$\beta = 99.7^\circ$			$\beta = 100.3^\circ$			
Resolution range (Å)	50-1.90 (1.97-1.90)	50-1.97 (2.06-1.97)	50-1.78 (1.84-1.78)	50-2.0 (2.07-2.00)	40-2.0 (2.11-2.00)	20-2.0 (2.07-2.00))	50-2.2 (2.28-2.20)	50-2.0 (2.07-2.00)
# of unique reflections	203,658 (18,439)	123,961 (11,025)	242,993 (24,075)	173,119 (17,129)	121,694 (17,141)	175,702 (17,360)	128,840 (12,713)	172,594 (17,108)
Completeness (%)	98.8 (90.3)	97.6(87.3)	99.9 (99.8)	100 (100)	98.1(95.3)	100 (100)	99.3 (98.8)	99.9 (100)
Redundancy	6.8 (4.4)	3.8 (3.7)	11.1 (10.0)	11.3 (11.2)	3.0(2.7)	7.3 (7.1)	11.3 (11.3)	11.2 (11.1)
Mean $I/\sigma(I)$	33.6 (2.8)	34.8 (10.6)	41.8 (5.6)	42.3 (9.5)	12.0 (3.1)	33.1 (6.2)	24.2 (2.9)	37.7 (6.5)
R_{merge}	0.064 (0.285)	0.056 (0.161)	0.079 (0.242)	0.070 (0.229)	6.8 (30.7)	0.072 (0.261)	0.118 (0.355)	0.080 (0.311)
twin factor	-	-	0.463	0.370	-	-	0.421	0.467
Refinement								
Resolution range (Å)	20-1.9	20-2.00	20-1.78	20-2.0	20-2.00	20-2.0	20-2.2	20-2.0
R -factor	0.192	0.197	0.235	0.199	0.198	0.199	0.206	0.235
R_{free}	0.207	0.229	0.258	0.216	0.231	0.217	0.236	0.259
average B-factor								
main chain atoms (Å ²)	28.3	22.1	22.0	19.1	26.6	24.1	38.7	27.8
side chain atoms (Å ²)	30.4	24.2	23.8	21.3	28.5	26.0	40.0	29.5
metal ions (Å ²)	26.4	29.4	31.0	28.0	41.4	22.2	37.0	25.9
binding ions or molecules to the active site (Å ²)	42.0 (inhibitor)	30.7 (cacodylate)	35.3 (cacodylate)	-	35.9 (chloride)	40.1 (substrate)	49.8 (chloride)	35.4 (chloride)
water molecules (Å ²)	35.7	29.5	31.6	25.8	30.2	30.4	42.0	33.9
RMSDs								
Bond lengths (Å)	0.005	0.005	0.006	0.005	0.005	0.005	0.006	0.006
Bond angles (deg.)	1.26	1.22	1.24	1.22	1.23	1.27	1.22	1.26

Values in parentheses refer to the last resolution shell. Through refinement procedure, occupancy of 1.0 was used for binding ions or molecules to the active site.